DNA 5618T

INJURIES PRODUCED BY THE PROPAGATION OF AIRBLAST WAVES THROUGH ORIFICES

Donald R. Richmond
E. Royce Fletcher
Keith Saunders
John T. Yelverton
Lovelace Biomedical and Environmental Research Institute
P.O. Box 5890
Albuquerque, New Mexico 87185

1 March 1980

Topical Report for Period 1 March 1979—1 March 1980

CONTRACT No. IACRO 81-832

THIS WORK SPONSORED BY THE DEFENSE NUCLEAR AGENCY
UNDER RDT&E RMSS CODE B384081466 U99QAXMK00008 H2590D.

Prepared for
Director
DEFENSE NUCLEAR AGENCY
Washington, D. C. 20305

Destroy this report when it is no longer needed. Do not return to sender.

PLEASE NOTIFY THE DEFENSE NUCLEAR AGENCY, ATTN: STTI, WASHINGTON, D.C. 20305, IF YOUR ADDRESS IS INCORRECT, IF YOU WISH TO BE DELETED FROM THE DISTRIBUTION LIST, OR IF THE ADDRESSEE IS NO LONGER EMPLOYED BY YOUR ORGANIZATION.

UNCLASSIFIED

SECURITY CLASSIFICATION OF THIS PAGE (When Data Entered)

REPORT DOCUMENTATION PAGE		READ INSTRUCTIONS BEFORE COMPLETING FORM
1 REPORT NUMBER DNA 5618T	2. GOVT ACCESSION NO.	3 RECIPIENT'S CATALOG NUMBER
4. TITLE (and Subtitle) INJURIES PRODUCED BY THE PROPAGATION OF AIRBLAST WAVES THROUGH ORIFICES		5 TYPE OF REPORT & PERIOD COVERED Topical Report for Period 1 Mar 79 – 1 Mar 80 6 PERFORMING ORG. REPORT NUMBER
7. AUTHOR(s) D. Richmond, E. R. Fletcher, K. Saunders and J. T. Yelverton		8 CONTRACT OR GRANT NUMBER(s) IACRO 81-832
9 PERFORMING ORGANIZATION NAME AND ADDRESS Lovelace Biomedical and Environmental Research Institute, P. O. Box 5890, Albuquerque, New Mexico 87185		10 PROGRAM ELEMENT, PROJECT, TASK AREA & WORK UNIT NUMBERS Subtask U99QAXMK000-08
11 CONTROLLING OFFICE NAME AND ADDRESS Director Defense Nuclear Agency Washington, D. C. 20305		12 REPORT DATE 1 March 1980 13 NUMBER OF PAGES 28
14 MONITORING AGENCY NAME & ADDRESS(if different from Controlling Office)		15 SECURITY CLASS. (of this report) UNCLASSIFIED 15a DECLASSIFICATION DOWNGRADING SCHEDULE

16. DISTRIBUTION STATEMENT (of this Report)

Approved for public release; distribution unlimited.

17. DISTRIBUTION STATEMENT (of the abstract entered in Block 20, if different from Report)

18 SUPPLEMENTARY NOTES

This work sponsored by the Defense Nuclear Agency under RDT&E RMSS Code B384081466 U99QAXMK00008 H2590D.

19. KEY WORDS (Continue on reverse side if necessary and identify by block number)

Blast Criteria	Airblast Jetting	Shocktubes
Blast Injuries	Personnel Effects	
Chamber Filling	Stagnation Overpressures	

20 ABSTRACT (Continue on reverse side if necessary and identify by block number)

The biological effects produced by airblast waves passing through small openings were evaluated using sheep. Specimens were oriented with their thoraces in front of circular orifices of 3.8- and 7.6-cm radii in the end-plate of a 0.6-m diameter shocktube. Subjects were also tested in front of a D-shaped orifice, equivalent radius of 24 cm, in the upstream wall of a test chamber located beyond the end of a 1.8-m diameter shocktube. The animals sustained crushing type of injuries, primarily to the rib cage, lungs, and liver.

DD FORM 1 JAN 73 1473 EDITION OF 1 NOV 65 IS OBSOLETE

UNCLASSIFIED

SECURITY CLASSIFICATION OF THIS PAGE (When Data Entered)

20. Abstract (Continued)

Stagnation overpressures were measured at various distances downstream from circular and rectangular orifices. Equations were developed to compute the stagnation overpressures as a function of input overpressures.

Injury levels were related to the stagnation overpressure and distance from the orifice. Based on these results, injury criteria were developed for personnel: no injury below 0.7, slight injury from 0.7 to 1.4, and severe injury above 1.4 atm of stagnation overpressure. The criteria were discussed in relation to the occupants of armored vehicles.

PREFACE

The information in this report should aid in defining the airblast hazards to personnel inside armored vehicles and certain field fortifications.

The research was performed under U. S. Department of Energy Contract No. EY-76-C-1013 through Interagency Agreement with the Defense Nuclear Agency, DNA RDT&E B384081466 U99QAXMK00008 H2590D and was performed for Director, Defense Nuclear Agency, Washington, D. C.

The authors wish to acknowledge the contributions of Mrs. Berlinda Martinez who provided editorial assistance and compiled this report and Mr. Takeshi Minagawa who prepared the illustrations.

This research was conducted according to the principles enunciated in the "Guide for Laboratory Animal Facilities and Care," prepared by the National Academy of Sciences, National Research Council.

CONVERSION FACTORS FOR METRIC (SI) TO U.S. CUSTOMARY
UNITS OF MEASUREMENT

Multiply	By	To Obtain
centimeters	0.3937008	inches
meters	3.280840	feet
square meters	10.76391	square feet
cubic meters	35.31467	cubic feet
kilometers	0.6213712	miles
meters per second	3.280840	feet per second
kilopascals	0.1450377	pounds-force per square inch (psi)

TABLE OF CONTENTS

LIST OF ILLUSTRATIONS

INTRODUCTION

The airblast hazard to personnel in open terrain was reported to depend on the peak overpressure, the duration of the overpressure, and the orientation of the subject with respect to the explosive source.[1] This applied, in general, to both the direct-overpressure effects and blast-displacement effects.

The response of personnel to airblast inside open field fortifications depended on the volume of the structure and the area of its entrance. Inside small structures with relatively large openings, such as foxholes and weapons emplacements, the direct-overpressure effects predominated because of the multiplication of the incident shock front when reflected from the walls and floor of the structure.[2]

Inside larger structures with door-size openings, for instance open shelters and command posts, the direct effects were less important since the peak pressures in the initial shock and subsequent reflections inside the structure were a small fraction of that in the outside wave. Blast-displacement effects predominated because during the fill phase the static pressure became converted to high-velocity flow through the entryway. Inside the doorway, the velocity of the entering flow was greater than that in the blast wave on the surface.

The airblast threat to personnel inside armored vehicles wherein the blast enters through open hatches and firing ports has not been defined. The purpose of this study was to determine injury levels produced by airblasts transmitted through small openings as a function of the input overpressure and distance from the openings.

PROCEDURES

SHOCKTUBES

Two shocktubes were used in this study to drive airblast waves through orifices.

One of the shocktubes was 45 m long with a 0.6 m I.D. (Figure 1). It was driven by compressed air and utilized Mylar® diaphragms. Endplates that contained a given size orifice were placed at the distal end of the expansion chamber. Circular orifices, 7.6- and 3.8-cm radii, and a rectangular orifice, 11.4 x 29.2 cm, were utilized. Most of the animal testing and overpressure measurements were done in connection with the 7.6-cm-radius orifice. The duration of the overpressure on the upstream side of the endplate was on the order of 200 msec.

The second shocktube was approximately 80 m long and varied from 1.0 to 1.8 m in diameter (Figure 1). It was operated with compressed air or by the detonation of

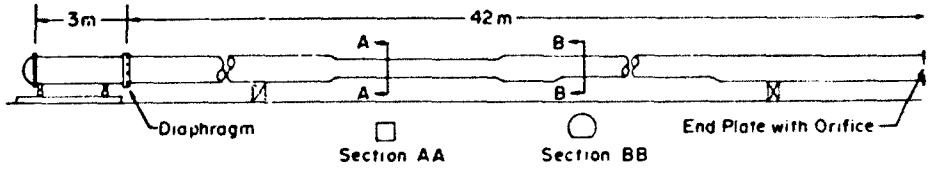

0.6m DIAMETER SHOCK TUBE

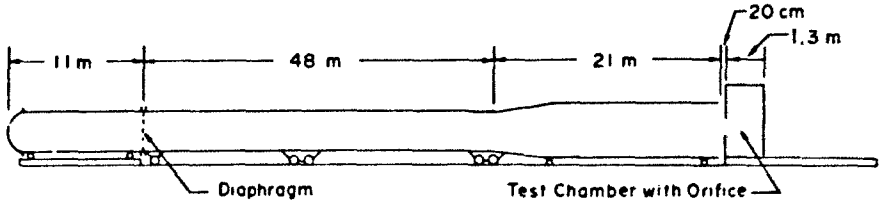

1.0—1.8 m DIAMETER SHOCK TUBE

Figure 1. Shocktube configurations.

hydrogen-oxygen mixtures in the compression chamber. Mylar® diaphragms were used. The shocktube was operated open-ended. A test chamber, 1.3 by 3.0 m and roughly semicircular in crossection, was located 20 cm from the end of the shocktube. The chamber had a volume of about 9 m^3. A D-shaped orifice was in the center of the upstream wall of the chamber. This orifice was patterned after the hatches in many armored vehicles. It had an area of 0.186 m^2 and an equivalent radius of 24 cm. Side-on overpressures were measured by transducers (Model ST-2, Susquehanna Instruments) 30 cm in from the end of the shocktube and at the center of the side wall inside the test chamber. Signals from the transducers were recorded by cathode ray oscilloscopes. Typical side-on overpressure patterns are illustrated in Figure 2. The duration of the overpressure in the shocktube averaged 190 msec; inside the test chamber it averaged 212 msec. Stagnation overpressures were not measured inside the test chamber.

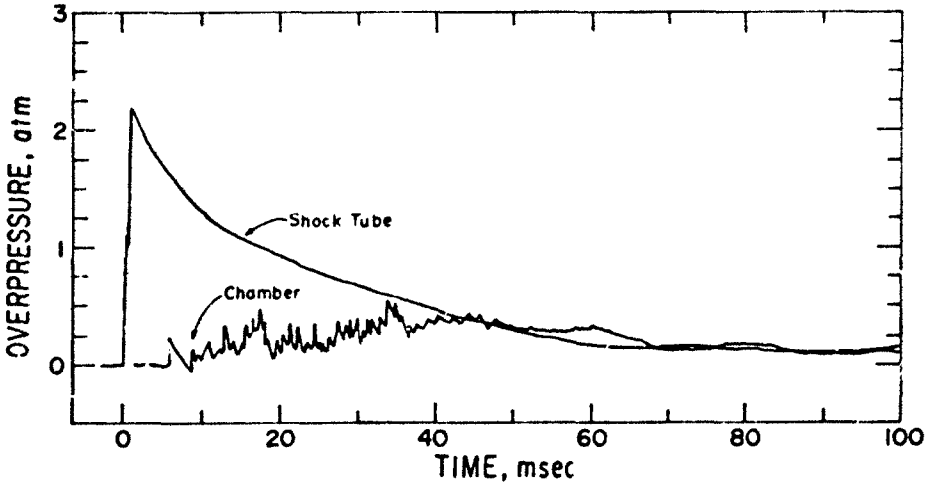

Figure 2. Pressure-time patterns measured at the end of the 1.0- to 1.8-m diameter shocktube and on the side wall of the test chamber.

TEST SUBJECTS

Female sheep, Columbia-Rambouillet cross, with a mean body weight of 41 kg, were used to assess the effects of airblast waves propagating through orifices. All animals were anesthetized by an intravenous injection of sodium pentobarbital. They were maintained at a surgical level of anesthesia from 5 minutes before each test until they were sacrificed within 30 minutes following the test. The experimental design was to determine no injury, slight injury, and severe injury levels in terms of distance from a 7.6-cm radius orifice for various input overpressure levels upstream of the orifice. A total of 21 sheep were tested at seven distances downstream of the 7.6-cm radius orifice. The subjects were restrained in a fixed chair with the ventral surfaces of their thoraces in line with the orifice.

Four unrestrained animals, numbered 27 through 30, were placed with the ventral surfaces of their thoraces 61 cm from the 7.6-cm-radius orifice. They were suspended by two lines attached to rings that could slide along an overhead pipe oriented parallel to the long axis of the shocktube. The blast-displacement time patterns of the subjects were measured by high-speed motion-picture cameras.

Five subjects were restrained in a chair with the ventral surfaces of their thoraces in line with the 3.8-cm radius orifice. The three at a distance of 30 cm received stagnation overpressures of from 2.30 to 2.84 atm. Those at 61 cm from the orifice were subjected to 1.36 and 1.75 atm.

Nine subjects were exposed to blast inside the test chamber. Eight were approximately 60 cm from the D-shaped orifice. Four were seated and restrained with the ventral surfaces of their thoraces in line with the orifice. Two were seated unrestrained with the right sides of their thoraces in line with the orifice. Three were suspended and oriented with their heads toward the orifice, long axis of their bodies parallel to the floor of the chamber. An additional subject was suspended with its head at the orifice.

RESULTS

STAGNATION OVERPRESSURES IN JETS EMANATING FROM ORIFICES

Circular Orifices

The atmospheric pressure into which the jet expanded outside the shocktube was 82.7 kPa. All pressures in this report were expressed in atmospheres. The peak reflected pressure on the upstream side of the endplate was designated as the input pressure, P_i. Stagnation pressures, designated P_s, were measured by face-on transducers at various distances, X, from the orifice and at various distances, Y, from the axis of the orifice.

Figure 3 illustrates the stagnation overpressure-time patterns measured at selected distances from the 7.6-cm radius orifice along the center axis. These waveforms were generated by input overpressures, P_i-1, of 0.80 atm. The waveforms were characterized by an initial shock front followed by a growth in the stagnation overpressure. There was a rapid decrease in the magnitude of the incident shock front with distance from the orifice and a corresponding increase in the time between the shock front and and the time to peak stagnation overpressure.

In general, for as long as the input overpressure was approximately constant, the recorded stagnation overpressure tended to remain constant, although moderately large fluctuations which appeared to be random in nature were noted (see Figure 3). Each P_i-1, X, and Y combination was tested at least two times, and an average stagnation overpressure was computed using the values obtained by averaging through the fluctuations on the individual records. In order to test scaling procedures, a limited number of measurements were made using a 3.8-cm radius orifice exposed to a P_i-1 of 3.50 atm.

Figure 4 shows, for a P_i-1 of 1.33 atm, the measured stagnation overpressures, P_s-1, as a function of the distances from the orifice and axis scaled in terms of the orifice radius. For some distance beyond the orifice, the stagnation overpressure remained nearly constant and equal to the input overpressure. The P_s-1 appeared to decrease smoothly with X, and, at a given X, P_s-1 was higher near the center of the orifice than it was near the edge.

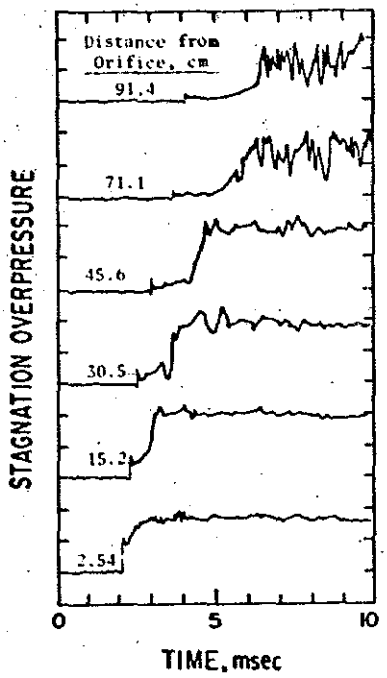

Figure 3. Pressure-time patterns measured by face-on gauges on the center axis at distances from the 7.6-cm radius orifice generated by input overpressures of 0.80 atm.

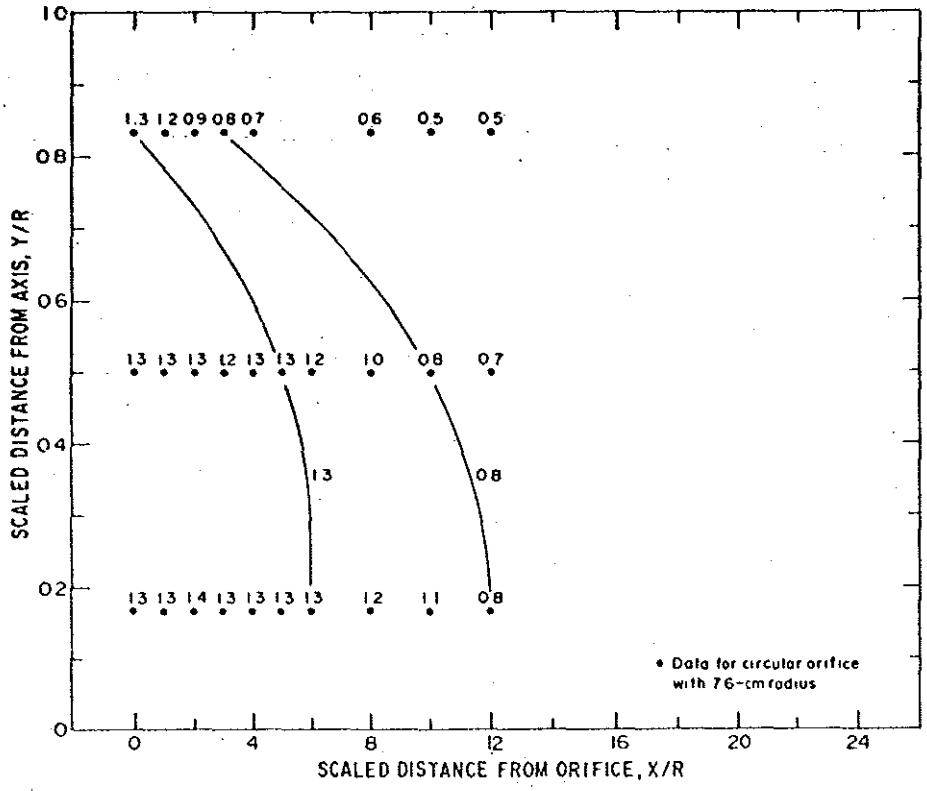

Figure 4. Stagnation overpressure contours from a 7.6-cm radius orifice generated by an input overpressure of 1.33 atm.

Figure 5 presents the stagnation overpressure contours for a P_i-1 of 3.50 atm. At the orifice (X/R = 0), the stagnation overpressure was approximately equal to the input overpressure of 3.50 atm. It can be seen that the stagnation overpressure appeared to go through a series of oscillations with distance. The stagnation overpressure appeared to be at a local maximum for X/R values of approximately 0.0, 3.0, and 6.0 and at a local minimum for X/R values of approximately 1.5 and 5.0. Thus, the length of one period represented approximately 3.0 to 3.3 radii. An empirical formula cited in Reference 4 for steady-state jets indicated that the period length expressed in radii was approximately equal to

$$1.78\ (P_i\text{-}1.9)^{1/2}$$

For a P_i-1 of 3.50 atm, this expression predicted a period length of 2.9 radii which was close to the value estimated from Figure 5 for transient jets.

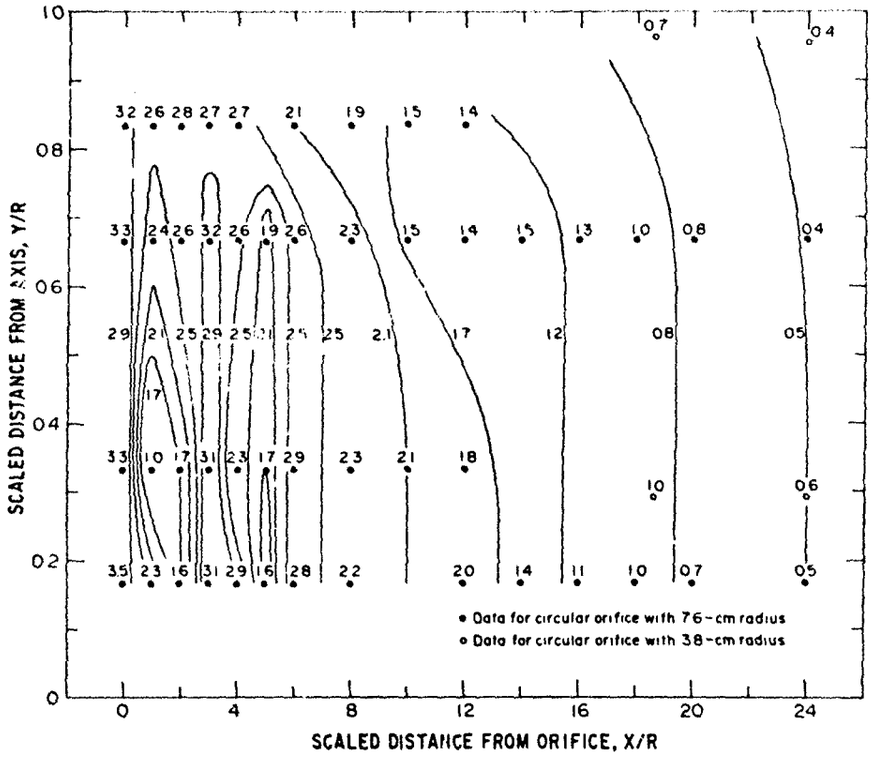

Figure 5. Stagnation overpressure contours from a 7.6-cm radius orifice generated by an input overpressure of 3.50 atm.

According to Figure 5, the stagnation overpressure, P_s-1, decreased smoothly with distance for X/R values greater than approximately six. At these distances, for a given X, P_s-1 was larger near the axis of the orifice than it was away from the axis.

For the various P_i-1 and X combinations tested, P_s-1 was measured at several Y/R values less than 1.0. By taking each P_s-1 value as the mean stagnation overpressure over an area in the shape of a two-dimensional torus, it was possible to compute the average stagnation overpressure over the projected orifice area for each X and P_i-1. These averaged stagnation overpressures were plotted in Figure 6 as a function of X/R for the four input overpressures. It was noted that the data for each input overpressure were approximately linear and could be represented by an equation of the form

$$P_s\text{-}1 = (P_{sm}\text{-}1)\left(1 - \frac{X/R}{X_m/R}\right) \qquad (1)$$

where P_{sm} was the maximum value of P_s (i.e., the P_s for X/R = 0) and X_m was the maximum value of X (i.e., the X for P_s-1 = 0). The P_{sm} values estimated by fitting lines to the data were close to the values that would be predicted from the theoretical Pitot-tube formula.[5]

$$P_{sm}\text{-}1 = P_i\text{-}1 \qquad \text{for } P_i < 1.893 \qquad (2)$$

$$P_{sm}\text{-}1 = 6\left[(P_i)^{2/7} - 1\right]^{7/2} / \left[(35/36)\,(P_i)^{2/7} - 1\right] 1 \quad \text{for } P_i \geq 1.893$$

Note that when the flow was subsonic (P_i <1.893), P_{sm} was equal to P_i, whereas when the flow became supersonic, these pressures differ as a result of the curved shock wave that forms in front of the gauge.

Least-squares regression lines were fitted to the data in Figure 6 subject to the constraint that P_{sm} corresponded to the theoretical value given by Equation 2. The X_m values were then computed from the regression equations. The following empirical equation was developed expressing X_m as a function of P_i:

$$X_m/R = \left[0.02905 + 0.02121\ (P_i-1)^{-0.8}\right]^{-1} \tag{3}$$

It should be noted that the P_i-1 values used to derive this equation ranged from 0.80 to 5.71. Since Equation 3 was empirical in nature, it would be suspect to use it to extrapolate beyond the experimental range. In particular, it is not known if X_m/R would approach an upper bound with increasing P_i as predicted by the formula.

The four lines in Figure 6 were derived from Formulas 1, 2, and 3 using the measured P_i-1 values. In general, the lines fit the data reasonably well. Note that the line for P_i-1 = 3.50 falls close to the data for either the 3.8- or the 7.6-cm radius orifice. Because the stagnation overpressure oscillated with distance from the orifice (see Figure 5), the data exhibit a large scatter around this line for X/R values less than 6. The dashed lines were drawn through the data to indicate the approximate nature of the oscillations. The Mach number, M, at any point in the undisturbed jet (the jet without the presence of gauges) can be estimated from the measured P_s-1 value at that point using the following formula.[5]

$$P_s-1 = (1 + M^2/5)^{7/2} - 1 \qquad \text{for } P_s < 1.893$$

$$P_s-1 = (6M^2/5)^{7/2}/(7M^2/6 - 1/6)^{5/2} - 1 \qquad \text{for } P_s > 1.893 \tag{4}$$

A Mach number scale derived from Formula 4 has been included in Figure 6.

Rectangular Orifice

A limited number of tests were conducted using an 11.4 x 29.2-cm rectangular orifice subjected to an input overpressure of 3.50 atm. On a given test, each of

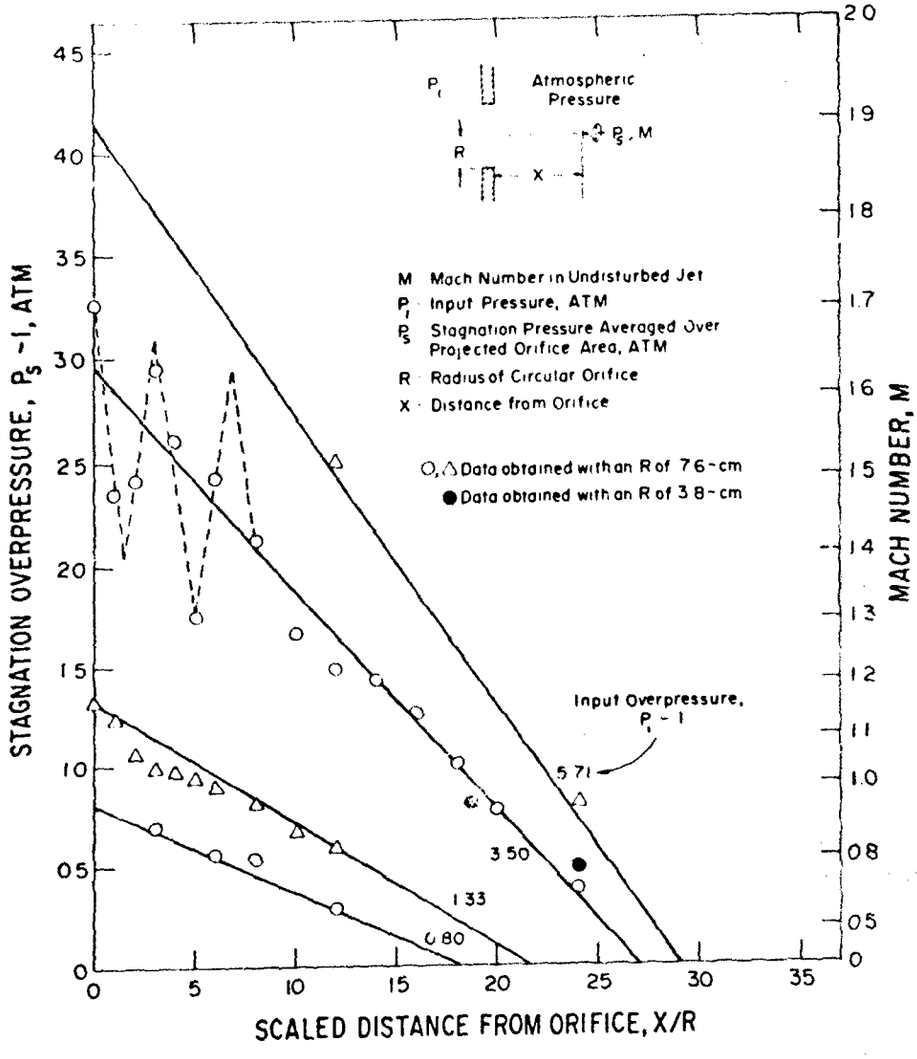

Figure 6. Stagnation overpressures averaged over the projected area of circular orifices.

the stagnation overpressure gauges was located an equal distance from the two short ends of the orifice with one gauge being 1.3 and the other being 3.8 cm from the orifice axis. The distance from the orifice to the gauges was varied on each test. The average stagnation overpressure over the projected orifice area was estimated to be 4/9 multiplied by the value measured at 1.3 cm plus 5/9 multiplied by the value measured at 3.8 cm. For a given distance from the orifice, the two measured stagnation overpressures never differed by more than 15 percent. For this reason, the computed average overpressures may be close to the true values even though they were based on a very limited number of measurements.

Figure 7 shows the data for the rectangular orifice in an analogous manner to the circular orifice shown in Figure 6. The figure was drawn using an equivalent R value assumed to be the radius of a circular orifice with an area equal to that of the rectangular orifice. The line in Figure 7 was the same regression line for a circular orifice that appeared in Figure 6. Except at X/R = 0, all of the data points fell below the line. For X/R values of less than 10, the measured stagnation overpressures, P_s-1, were on the average 0.85 times as large as the overpressures predicted from the line using the same X/R values. By way of comparison, a corresponding value of 0.97 was obtained for X/R values less than 10 using the circular orifice data for a P_i-1 of 3.50 atm. Thus, for a P_i-1 of 3.50 atm and X/R values less than 10, the average stagnation overpressures for a rectangular orifice can reasonably be approximated by taking 0.85 times the average overpressure predicted for a circular orifice. It is not certain if such a decrease in pressure would be appropriate at larger values of X/R, in that the datum point on Figure 7 at X/R = 14 fell close to the line.

The dashed lines drawn in Figure 7 indicated that, as in the case of a circular orifice exposed to the same P_i-1 of 3.50 atm, the stagnation overpressure tended to oscillate with the distance from the rectangular orifice. The length of one period appeared to be about 2.5 equivalent radii, somewhat less than the 3.0 to 3.3 radii found for a circular orifice.

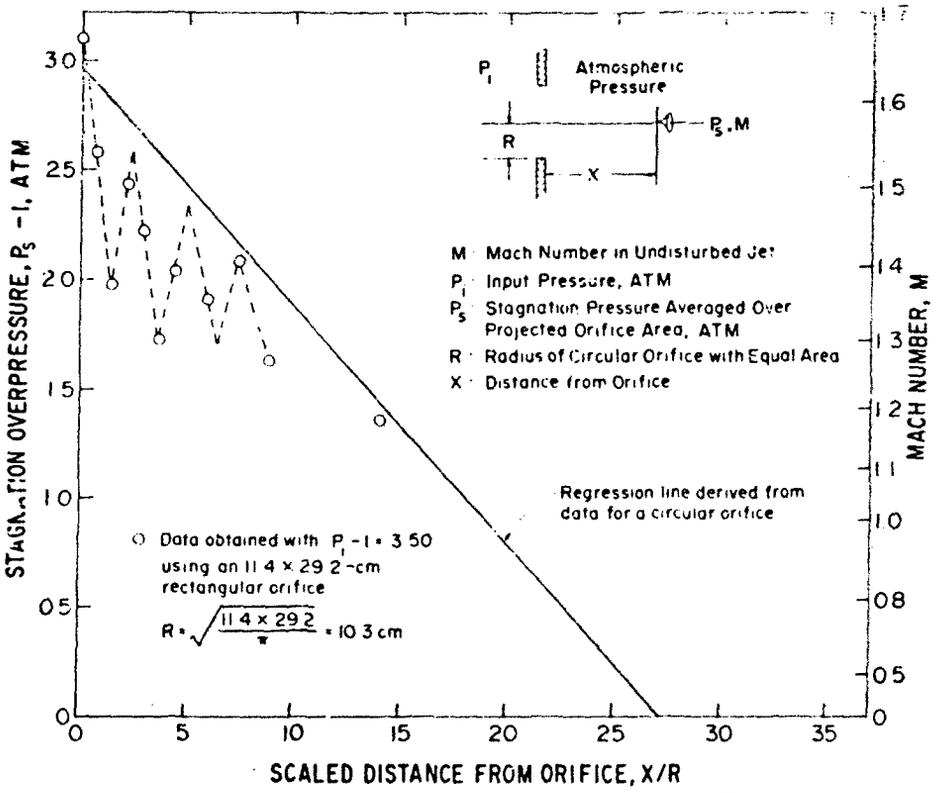

Figure 7. Stagnation overpressures averaged over the projected area of a rectangular orifice.

NATURE OF INJURIES

Crushing type of injuries were produced by the airblast jet emanating from the orifices. Among the animals in front of the 7.6-cm orifice, the intrathoracic injuries ranged from contusions of the intercostal muscles to multiple compound rib fractures along the midaxillary line and/or at the vertebral junction. In severe cases, the ends of fractured ribs punctured the lungs producing massive hemothoraces. The pulmonary lesions ranged from small subpleural air blebs surrounded by petechial hemorrhages to multiple, large air blebs and associated hemorrhagic areas. Scattered contusions of the diaphragm were a common lesion. At the higher stagnation overpressure levels this lesion was severe. Intra-abdominally ruptured livers with associated hemoperitoneum were a common finding.

The same injury pattern described above was found in subjects that were unrestrained in front of the 7.6-cm radius orifice. According to the film records, the thoraces of restrained or unrestrained animals underwent marked compression during the blast loading. Maximum compression occurred within the same time period in both groups. The thoraces of unrestrained animals would reach their maximum compression before the animals were displaced a distance of 10 cm by the flow. The peak velocity attained by Animals Nos. 27, 28, 29, and 30 was 4.27, 2.68, 1.37, and 7.92 m/sec, respectively.

The animals restrained at distances of 30 and 61 cm in front of the 3.8-cm radius orifice were not significantly injured by input pressures that produced severe injury in subjects at comparable distances from the 7.6-cm radius orifice.

Inside the test chamber, the same crushing injuries occurred in animals seated with their thoraces facing or side-on to the orifice as occurred in connection with the 7.6-cm radius orifice. Animals oriented with their heads toward the orifice were less injured than those with their thoraces opposite the orifice.

INJURIES IN RELATION TO STAGNATION OVERPRESSURE

Figure 8 summarizes the degree of injury for each animal as a function of the stagnation overpressure and scaled distances from the 7.6- and 24.4-cm radius orifices. The symbols indicate animals with no injuries, those with slight injuries, and those with severe injuries. Slight injuries included small subpleural air blebs on the lungs, traces of lung hemorrhage, and mild intercostal contusions. The severe injuries were, for the most part, in the form of rib fracture, liver rupture, and extensive contusion of the diaphragm. As seen in Figure 8, the no-injury region was below 0.7 atm of stagnation overpressure and slight injuries occurred between 0.7 and 1.4 atm. Above 1.4 atm all the animals sustained severe injuries. Animal No. 2 was a 3-minute fatality.

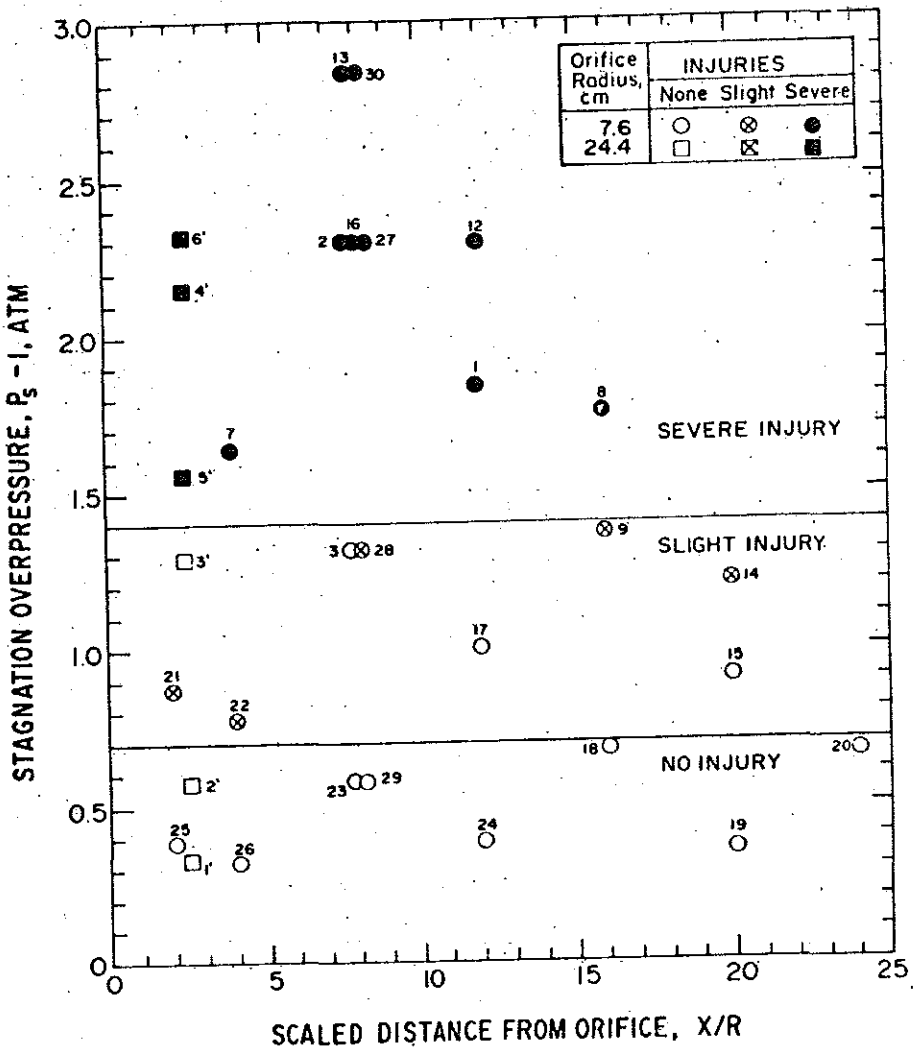

Figure 8. Injury levels in relation to stagnation overpressures and distance from orifices.

DISCUSSION

INJURY CRITERIA FOR BLAST-INDUCED JET FLOW THROUGH ORIFICES

The stagnation overpressure-injury levels obtained with sheep were selected as injury criteria for personnel subjected to blast jet flow from orifices. The tentative criteria were applied to personnel inside armored vehicles when their thoraces were in line with an opening, Figure 9. The curves related the incident side-on overpressures required to generate stagnation overpressure levels through orifices of 0.7 and 1.4 atm as a function of range and explosive yield. The criteria apply to openings in vehicles that were side-on or back-on to the blast. The upper curve in the figure pertains to openings that were in the portion of the vehicle oriented face-on to the blast and thus were filled by reflected overpressures.

The criteria apply to circular orifices of from 15 to 48 cm in diameter, to square openings having an equivalent area, and to rectangular ones having L/W ratios of 2.5 or less. The criteria do not apply to openings of less than 15 cm in diameter.

Certain areas were identified that require better definition before more generalized blast criteria can be established. Among these were the influence that the duration of the jet flow had on the biological effects and the lateral extent of the jet flow through openings at the higher overpressure levels. The response of the head and neck to the blast jet flow and an assessment of the effects produced by jets downstream of rectangular openings having large L/W ratios were other areas that required further definition.

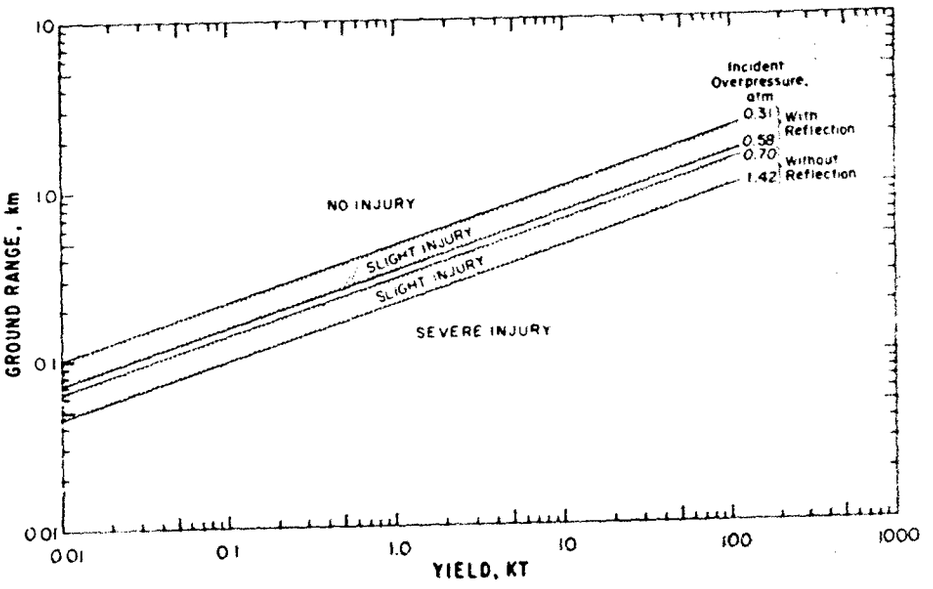

Figure 9. Injury criteria for blast-induced jet flow through orifices in relation to range and yield computed for a surface burst.

REFERENCES

1. White, C. S., R. K. Jones, E. G. Damon, E. R. Fletcher and D. R. Richmond, "The Biodynamics of Air Blast," Technical Progress Report, DNA 2738T, Defense Nuclear Agency, Department of Defense, Washington, D. C., July 1971.

2. Richmond, D. R., E. R. Fletcher and R. K. Jones, "Project LN401—Blast Protection Afforded by Foxholes and Bunkers," in Event Dial Pack Symposium Report, March 30-April 2, 1971, Vol. II, pp. 581-606, The Technical Cooperation Program, The Defence Research Board of Canada, Ottawa, Ontario, Canada, March 1971.

3. Fletcher, E. R., D. R. Richmond, R. O. Clark and J. T. Yelverton, "Blast Displacement in Field Fortifications," in Proceedings of the Dice Throw Symposium, Vol. 3, Section 29, DNA 4377P-3, Department of Defense, Defense Nuclear Agency, Washington, D. C., July 1977.

4. Pai, S-I, Fluid Dynamics of Jets, D. Van Nostrand Company, Inc., New York, New York, 1954.

5. Shapiro, A. H., The Dynamics and Thermodynamics of Compressible Fluid Flow, Vol. I, The Ronald Press Company, New York, New York, 1953.

DISTRIBUTION LIST

DEPARTMENT OF DEFENSE

Armed Forces Radiobiology Rsch Inst
ATTN: Director

Armed Forces Staff College
ATTN: Ref & Tech Svcs Br

Assistant Secretary of Defense
International Security Affairs
ATTN: European & NATO Affairs
ATTN: Policy Plans & NSC Affairs

Assistant Secretary of Defense
Comm, Cmd, Cont & Intell
ATTN: Surv & Warn Sys

Assistant to the Secretary of Defense
Atomic Energy
ATTN: Executive Assistant

Command & Control Technical Center
ATTN: C-312
ATTN: C-343
ATTN: C-332
ATTN: C-315

Commander-in-Chief, Atlantic
ATTN: N-22

Commander-in-Chief, Pacific
ATTN: J-32
ATTN: J-54
ATTN: J-634

Defense Intelligence Agency
ATTN: DIA/VPA-2
ATTN: DB-6
5 cy ATTN: DB-4

Defense Nuclear Agency
ATTN: STNA
ATTN: NATD
ATTN: NATA
4 cy ATTN: TITL

Defense Technical Information Center
12 cy ATTN: DD

Field Command
Defense Nuclear Agency
ATTN: FCP

Field Command
Defense Nuclear Agency
Livermore Branch
ATTN: FCPRL

Intelligence Center, Pacific
ATTN: COMIPAC

Interservice Nuclear Weapons School
ATTN: TTV

DEPARTMENT OF DEFENSE (Continued)

Joint Chiefs of Staff
ATTN: SAGA/SSD
ATTN: J-3, Strat Op Div
ATTN: J-3
ATTN: J-5, Nuclear Div
ATTN: J-5, Strategy Div, W. McClain
ATTN: SAGA/SFD

Joint Strate Tgt Planning Staff
ATTN: JP
ATTN: JLA
ATTN: JL
2 cy ATTN: JLTW-2

National Defense University
ATTN: NWCLB-CR
ATTN: ICAF Tech Lib

Director
NET Assessment
Office of the Secretary of Defense
ATTN: Mil Assts

U.S. European Command
ATTN: J-2
ATTN: J-5NPG
ATTN: J-3
ATTN: J-LW
ATTN: J-2-ITD
ATTN: J-6

U.S. National Military Representative
SHAPE
ATTN: U.S. Documents Officer

Under Secretary of Defense for Rsch & Engrg
ATTN: OUSDRE, Rsch & Adv Tech Tac War Prog

Deputy Assistant Secretary of Defense
Energy, Environment & Safety
ATTN: DASD, EE&S

DEPARTMENT OF THE ARMY

Deputy Chief of Staff for Ops & Plans
Department of the Army
ATTN: DAMO-ZXA
ATTN: DAMO-NC

Harry Diamond Laboratories
Department of the Army
ATTN: DELHD-N-P

U.S. Army Armor School
ATTN: Tech Lib

U.S. Army Ballistic Research Labs
ATTN: DRDAR-TSB-S
ATTN: DRDAR-BLT, Effects Analysis Br

DEPARTMENT OF THE ARMY (Continued)

U.S. Army Cmnd & Gen Staff College
ATTN: ACQ, Lib Div

U.S. Army Concepts Analysis Agency
ATTN: CSSA-ADL

Commander-in-Chief
U.S. Army Europe and Seventh Army
ATTN: AEAGE
ATTN: AEAGC

U.S. Army Nuclear & Chemical Agency
ATTN: Library

U.S. Army TRADOC Sys Analysis Actvy
ATTN: ATAA-TAC

U.S. Army War College
ATTN: Library

U.S. Military Academy
ATTN: Document Lib

U.S. Army Medical R&D Cmd
ATTN: SGRD-SD

U.S. Army Chemical School
ATTN: ATZA-CM-AL

Water Reed Army Med Center
ATTN: Library

DEPARTMENT OF THE NAVY

Naval Postgraduate School
ATTN: Code 1424, Library

Naval Research Lab
ATTN: Code 1240

Naval Sea Systems Command
ATTN: SEA-643
ATTN: SEA-09G53

Naval Surface Weapons Center
ATTN: Code F31

Naval War College
ATTN: Doc Control

Nuclear Weapons Tng Gp, Pacific, Dept of the Navy
ATTN: Doc Control

Nuclear Weapons Tng Gp, Atlantic, Dept of the Navy
ATTN: Doc Control

Office of Naval Research
ATTN: Tech Info Svcs

Bureau of Medicine and Surgery
Department of the Navy
ATTN: NM&S-3C72
ATTN: NM&S-00
ATTN: NM&S-09

Naval Medical Rsch Inst
ATTN: Tech Ref Lib

DEPARTMENT OF THE NAVY (Continued)

National Naval Med Center
ATTN: Med Lib

DEPARTMENT OF THE AIR FORCE

Air Force School of Aerospace Med
ATTN: Radiobiology Div

Air Force Systems Command
ATTN: XR
ATTN: DL
ATTN: SD
ATTN: SCL-4

Air Force Weapons Lab
Air Force Systems Command
ATTN: SUL

Air University Library
Department of the Air Force
ATTN: AUL-LSE

Assistant Chief of Staff
Intelligence
Department of the Air Force
ATTN: INA

Deputy Chief of Staff
Research, Dev, & Acq
Department of the Air Force
ATTN: AFRDQI

Foreign Technology Div
Air Force Systems Command
ATTN: TQTM
ATTN: SDN
ATTN: CCN

Strategic Air Command
Department of the Air Force
ATTN: ADWN
ATTN: NRI, STINFO Lib
ATTN: DO
ATTN: XP
ATTN: NR

U.S. Air Force, Pacific
ATTN: XP

Commander-in-Chief
U.S. Air Forces in Europe
ATTN: USAFE/DEX

Commander-in-Chief
U.S. Air Forces in Europe
ATTN: USAFE/DOT

Commander-in-Chief
U.S. Air Forces in Europe
ATTN: USAFE/INA

Commander-in-Chief
U.S. Air Forces in Europe
ATTN: USAFE/INT

Commander-in-Chief
U.S. Air Forces in Europe
ATTN: USAFE/XPX

DEPARTMENT OF THE AIR FORCE (Continued)

U.S. Air Force Occupational & Env Health Lab
ATTN: CC
ATTN: TSNTPR

DEPARTMENT OF ENERGY

Department of Energy
Albuquerque Op Ofc
ATTN: CTID

Lovelace Biomed & Env Rsch Inst, Inc
4 cy ATTN: E. Fletcher
4 cy ATTN: K. Saunders
4 cy ATTN: J. Yelverton
4 cy ATTN: D. Richmond

OTHER GOVERNMENT AGENCIES

Central Intelligence Agency
ATTN: OSWR/NED

Federal Emergency Management Agency
National Sec Ofc Mitigation & Rsch
ATTN: Dep Dir, J. Nocita
ATTN: Asst Associated Dir

Department of State
Office of International Sec Policy
ATTN: PM/ISP

DEPARTMENT OF ENERGY CONTRACTORS

Lawrence Livermore National Lab
ATTN: Tech Info Dept, Lib

Los Alamos Nat Scientific Lab
ATTN: MX 364
ATTN: M/S634, T. Dowler

DEPARTMENT OF DEFENSE CONTRACTORS

Advanced International Studies Inst
ATTN: M. Harvey

Advanced Research & Applications Corp
ATTN: Doc Control

Aerospace Corp
ATTN: Library

BDM Corp
ATTN: J. Braddock

General Electric Co
ATTN: R. Minckler

General Research Corp
ATTN: Tac Warfare Op

Hudson Institute, Inc
ATTN: H. Kahn

IIT Research Inst
ATTN: Doc Lib

Institute for Defense Analyses
ATTN: Class Lib
ATTN: J. Grote

DEPARTMENT OF DEFENSE CONTRACTORS (Continued)

JAYCOR
ATTN: R. Sullivan

Kaman Sciences Corp
ATTN: T. Shelton

Kaman Sciences Corp
ATTN: E. Daugs

Kaman Tempo
ATTN: DASIAC

Martin Marietta Corp
ATTN: F. Marion

Pacific-Sierra Research Corp
ATTN: H. Brode
ATTN: G. Lang

Pacific-Sierra Research Corp
ATTN: D. Gormley

R & D Associates
ATTN: R. Port
ATTN: P. Haas
2 cy ATTN: Doc Con
2 cy ATTN: S. Borjon

R & D Associates
ATTN: J. Thompson

Santa Fe Corp
ATTN: D. Paolucci

Science Applications, Inc
ATTN: J. Warner
ATTN: Doc Control
ATTN: M. Drake

Science Applications, Inc
ATTN: W. Layson
ATTN: Doc Control

Science Applications, Inc
ATTN: L. Goure
ATTN: D. Kaul

System Planning Corp
ATTN: J. Douglas

T. N. Dupuy Associates, Inc
ATTN: T. Dupuy

Tetra Tech, Inc
ATTN: F. Bothwell

TRW Defense & Space Sys Group
ATTN: N. Lipner

TRW Defense & Space Sys Group
ATTN: P. Dai